Heliyon 10 (2024) e32289

Contents lists available at ScienceDirect

Heliyon

journal homepage: www.cell.com/heliyon

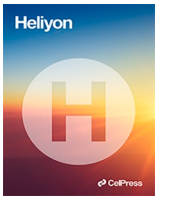

Research article

Unveiling a cuproptosis-related risk model and the role of FARSB in hepatocellular carcinoma

Junlin Duan [a], Xuan Zhang [b], Jingyu Xu [c], Jun Liu [a,1,**], Hetong Zhao [b,1,*]

[a] Department of Clinical Laboratory, Dongguan Hospital of Guangzhou University of Chinese Medicine, Dongguan, China
[b] Department of Traditional Chinese Medicine, Navy NO.905 Hospital, Navy Medical University, Shanghai, China
[c] Department of Traditional Chinese Medicine, Changzheng Hospital, Navy Medical University, Shanghai, China

ARTICLE INFO

Keywords:
Hepatocellular carcinoma
Cuproptosis
Gene signature
FARSB
Biomarker

ABSTRACT

Background: Cuproptosis, a type of regulated cell death that was recently identified, has been linked to the development of a variety of diseases, among them being cancers. Nevertheless, the prognostic significance and therapeutic implications of the cuproptosis potential index in hepatocellular carcinoma (HCC) remain uncertain.

Methods: Single-sample gene set enrichment analysis (ssGSEA) and Weighted Gene Co-expression Network Analysis (WGCNA) methodology was conducted to ascertain the identification of modular genes that are closely linked to cuproptosis. In addition, the gene signature indicative of prognosis was formulated by employing univariate Cox regression analysis in conjunction with a random forest algorithm. The efficacy of this gene signature in predicting outcomes was confirmed through validation in both The Cancer Genome Atlas (TCGA) and International Cancer Genome Consortium (ICGC) datasets. Furthermore, a study was undertaken to evaluate the association between the risk score and various clinical-pathological characteristics, explore the biological processes linked to the gene signature, and analyze tumor mutational burden and somatic mutations. Lastly, potential drugs targeting the identified gene signature were identified through screening.

Results: The results of our comprehensive analysis across multiple cancer types demonstrated a positive correlation between an elevated cuproptosis potential index (CPI) and an accelerated rate of tumor progression. Furthermore, employing the WGCNA technique, we successfully identified 640 genes associated with cuproptosis. Among these genes, we meticulously screened and validated a seven-gene signature (TCOF1, NOP58, TMEM69, FARSB, DHX37, SLC16A3, and CBX2) that exhibited substantial prognostic significance. Using the median risk score, the division of HCC patients into cohorts with high- and low-risk highlighted significant disparities in survival results, wherein the group with higher risk exhibited a less favorable overall survival. The risk score exhibited commendable predictive efficacy. Moreover, the *in vitro* knockdown of FARSB significantly hindered cell viability, induced G1 phase arrest, increased apoptosis, and impaired migration in HepG2 and Huh7 cells.

Conclusion: Our research has successfully identified a strong seven-gene signature linked to cuproptosis, which could be utilized for prognostic evaluation and risk stratification in patients

* Corresponding author. Navy NO.905 Hospital, Navy Medical University, Shanghai 200052, China.
** Corresponding author. Dongguan Hospital of Guangzhou University of Chinese Medicine, Dongguan 523127, China.
E-mail addresses: 12jliu3@alumni.stu.edu.cn (J. Liu), zht@smmu.edu.cn (H. Zhao).
[1] Jun Liu and Hetong Zhao contributed equally to this work and are the corresponding authors.

https://doi.org/10.1016/j.heliyon.2024.e32289
Received 27 January 2024; Received in revised form 30 May 2024; Accepted 31 May 2024
Available online 4 June 2024
2405-8440/© 2024 The Authors. Published by Elsevier Ltd. This is an open access article under the CC BY-NC-ND license (http://creativecommons.org/licenses/by-nc-nd/4.0/).

with HCC. Furthermore, the discovered gene signature, coupled with the functional analysis of FARSB, presents promising prospects as potential targets for therapeutic interventions in HCC.

1. Introduction

Hepatocellular carcinoma (HCC) is globally recognized as the second most prevalent source of cancer-associated fatalities, representing one-tenth of all such deaths worldwide [1]. Within China, which represents a high-risk area, approximately 55 % of liver cancer patients reside. The majority of HCC, the predominant form of liver cancer, arises from chronic liver inflammation (hepatitis) or metabolic abnormalities [2]. Although we've seen considerable progress in therapeutic strategies during the recent years, the outlook for advanced HCC continues to be disappointing [3,4]. Hence, thorough investigations into novel therapeutic targets and biological mechanisms have paramount importance in enhancing HCC treatment outcomes.

Emerging evidence suggests that disruption of copper homeostasis can contribute to cytotoxicity and impact tumor growth and metastasis [5,6]. Numerous studies have consistently shown elevated levels of copper in serum or tissues of various human cancers, including breast, lung, and liver cancers [7–9]. It is widely considered that the imbalance of copper concentrations in cancer significantly contributes to the stimulation of tumor development and advancement of the disease [10,11]. Copper serves as a crucial component for a number of enzymes participating in angiogenesis, cell proliferation, and tumor invasion [12]. Excessive copper accumulation can result in oxidative stress, DNA damage, and the promotion of pro-tumorigenic pathways [13]. In breast cancer, elevated copper levels have been associated with aggressive tumor characteristics and poorer prognosis [14,15]. Similarly, in brain tumors, increased copper levels correlate with tumor grade and invasiveness [16]. Prostate cancer cells also exhibit altered copper metabolism, which contributes to their survival and resistance to therapy [17]. Additionally, elevated copper levels have been observed in colon, lung, and liver cancers, suggesting their involvement in these malignancies as well [18,19].

Over the past few years, we have observed a considerable surge in the discovery of regulated cell death mechanisms, including necroptosis, ferroptosis, alkaliptosis, oxeiptosis, pyroptosis [20,21]. The pioneering article by Tsvetkov et al. published in the journal Science focused on the investigation of a unique form of cell death, termed 'cuproptosis,' that is induced by copper [22]. Cuproptosis primarily occurs through proteolipidation within mitochondria and is induced by copper [23,24]. Mechanistically, copper reduction occurs via direct interaction with lapidated constituents of the tricarboxylic acid (TCA) cycle. Enhanced lipidation of TCA enzymes, notably pyruvate dehydrogenase (PDH) complex, during the process of respiration leads to anomalous clustering of lipid-modified proteins and ensuing reduction of proteins containing Fe–S clusters. This ultimately leads to the development of acute proteotoxic stress, resulting in the ultimate demise of the cell. It is important to note that cuproptosis represents a distinctive method of cell death that relies on copper and lipidation processes. The complex interaction between copper, mitochondrial functions, and lipid metabolism contributes to the pathogenesis of cuproptosis. Further elucidation of these mechanisms deepens our comprehension of the regulatory networks implicated in this type of cell death and offers potential opportunities for therapeutic interventions. Further research is imperative for a comprehensive understanding of the complex molecular mechanisms involved in cuproptosis and its relevance to HCC. Moreover, the exploration of therapeutic strategies that specifically target the copper-lipidation axis holds promise for the mitigation or prevention of cuproptosis-induced damage and associated pathological conditions.

Recent advancements in the understanding of cell death pathways have highlighted the role of cuproptosis in cancer biology, yet its specific implications in hepatocellular carcinoma remain underexplored. This study addresses this gap by examining the impact of cuproptosis and its regulation by FARSB, providing insights into potential therapeutic targets that were previously unrecognized in the context of HCC. By focusing on this novel aspect, our work seeks to contribute to a more nuanced understanding of tumor biology and treatment resistance in liver cancer. Within the scope of this investigation, we utilized the HCC gene expression datasets from The Cancer Genome Atlas (TCGA) and International Cancer Genome Consortium (ICGC) to construct a personalized prognostic marker grounded on cuproptosis. By integrating the gene expression data with cuproptosis-related information, we identified a set of genes that held substantial association with the prognosis in HCC. These genes were utilized to assemble an individualized prognostic signature, which allowed for the stratification of HCC patients into different risk groups based on their predicted prognosis. Through comprehensive analysis and statistical evaluation, we demonstrated that our prognostic signature based on cuproptosis effectively predicted the prognosis. These findings highlight the clinical utility of cuproptosis-related genes as biomarkers for HCC prognosis prediction. The development of personalized prognostic signatures holds promise for improving patient management by facilitating tailored treatment strategies and enhancing therapeutic decision-making.

2. Materials and methods

2.1. Data sources

In this study, we developed a prognostic gene signature using gene expression data and corresponding clinical data from 365 HCC samples from TCGA dataset. To validate the reproducibility and robustness of our prognostic gene signature, we further analyzed 232 HCC samples from the ICGC dataset. Each dataset was employed with appropriate statistical methods to account for differences in sample size and demographic characteristics. The analysis in the later stage was exclusively conducted using the TCGA cohort data, which had the largest sample size. Ethical approval was not required for this secondary analysis.

2.2. Functional annotation and pathway analysis

The single-sample Gene Set Enrichment Analysis (ssGSEA) technique was applied to identify the key hallmark pathways [25]. Utilizing the clusterProfiler package, we performed the functional annotation of hub genes [26]. A significance threshold of $P < 0.05$ was deemed to suggest meaningful enrichment within both the Gene Ontology (GO) and Kyoto Encyclopedia of Genes and Genomes (KEGG) databases.

3. WGCNA

The Weighted Gene Co-expression Network Analysis (WGCNA) was performed to develop a co-expression network. After evaluating the quality of the expression matrix, we used the WGCNA package in R to determine the soft threshold, choosing $\beta = 4$ to build a scale-free network. Key modules were identified by setting the minimum module size as 30 and the MEDissThres as 0.25.

3.1. Identification of a potential prognostic signature

In this study, we initially conducted univariate Cox regression analysis with a threshold of $p < 0.01$ to identify candidate genes significantly associated with the prognosis of HCC patients. Cox regression is a crucial statistical method in survival analysis for evaluating the impact of covariates on survival time. Subsequently, we employed the Random Forest algorithm to assess the feature importance of these candidate genes. This assessment is based on the contribution of genes within each decision tree, and by aggregating the evaluation results from all trees, an overall importance score is obtained for each gene. Based on these scores, we identified the top 10 "hub genes" that contribute most significantly to model prediction. These pivotal genes were then used to construct a risk scoring model as follows: Risk score $= \beta_1 x_1 + \beta_1 x_1 + \beta_1 x_1 + \ldots + \beta_N x_N$ where N is the number of genes selected by Random Forest algorithm, x represents the gene expression value, and β is the gene coefficient determined in Cox regression analysis. Log-rank p-values were employed in Kaplan-Meier (K-M) analysis to identify the optimal gene combination or the final signature.

3.2. CIBERSORT analysis, tumor mutational burden value calculation and prediction of potential compounds

The CIBERSORT method was performed to estimate the proportion of immune cell types in a mixed cell population online [27].

Tumor Mutational Burden (TMB) analysis is a technique utilized to evaluate the overall mutation count in a tumor's genome, providing a measurement of mutations for each megabase of DNA in the tumor tissue while omitting synonymous mutations [28].

To predict the potential compounds that could be employed in HCC treatment, we determined the IC50 values of the compounds sourced from the Genomics of Drug Sensitivity in Cancer (GDSC; https://www.cancerrxgene.org) [29].

3.3. Cell culture and transfection

The HCC-derived cell lines HepG2, Huh7, and HCCLM3, as well as the normal liver cell line L02, were procured from the American Tissue Culture Collection (ATCC) and employed for *in vitro* experimentation. Cell culture media were obtained from Servicebio (Wuhan, China). Cells were transfected with short hairpin RNA (shRNA) molecules targeting FARSB. Lipo3000 (Invitrogen) was used to transfect the plasmids into cells. The shRNA sequences are as follows: NC-shRNA, gTTCTCCGAACGTGTCACGTttcaagagaACGTGACACGTTCGTTCGGAGAAttttt; FARSB shRNA-1, gCGAAGAATTTGATGAACTAttcaagagaT
AGTTCATCAAATTCTTCGttttt; FARSB shRNA-2, gGCTCCTCCCTAGAAATCAA
ttcaagagaTTGATTTCTAGGGAGGAGCttttt; FARSB shRNA-3, gAGAAGATATTGC.
TGATAAAttcaagagaTTTATCAGCAATATCTTCTttttt.

3.4. Western blot

The levels of FARSB expression in HCC cells (HepG2, Huh7, and HCCLM3) and normal liver cells (LO2) were assessed through Western blot analysis. Proteins were extracted, quantified, and separated by SDS-PAGE (wanleibio, China) before being transferred to PVDF (wanleibio, China) membranes. Membranes were probed with specific primary antibodies followed by HRP-conjugated secondary antibodies (wanleibio, China). The protein bands were visualized using an enhanced chemiluminescence (ECL) system (wanleibio, China), and the resulting images were captured utilizing a chemiluminescence imaging system. FARSB antibody was from Affinity biosciences and β-actin antibody was from wanleibio.

3.5. Real-time PCR analysis

Total RNA was extracted from HepG2 and Huh7 cells, both with and without FARSB knockdown, and reverse transcribed into cDNA. Real-time PCR was performed using SYBR Green PCR Master Mix. The expression of target genes was normalized to the expression of the housekeeping gene GAPDH, and relative gene expression was calculated using the 2ˆ-ΔΔCt method, with normalization to the expression of the housekeeping gene. The sequences of primers used are the following: FARSB F: GCTGCTGAAGTGGTTT, FARSB R: TCTGGTTGGAGGGATT, β-actin F: β-actin F, β-actin R: TAGAAGCATTTGCGGTGG.

3.6. Cell viability and apoptosis assays

The Cell Counting Kit-8 (CCK-8) assay was used to assess cell viability, and an apoptosis assay was used to evaluate the proportion of apoptotic cells. CCK8 kit was purchased from wanleilab. A plate cloning experiment was used to detect cell proliferation.

3.7. Cell cycle and migration assays

Flow cytometry was employed for cell cycle analysis, and wound-healing assays were used to assess cell migration. Cell cycle detection was performed using a kit purchased from wanleilab.

3.8. Statistical analysis

All statistical analyses were conducted using R software (version 4.1.0). The Student's t-test, ANOVA, Pearson's correlation coefficient, and chi-square or Fisher's exact tests were used as appropriate. A P-value less than 0.05 was considered statistically significant. Univariate and multivariate Cox regression analyses were executed to determine the prognostic value of our risk model in TCGA and ICGC cohorts. Additionally, time-dependent concordance-index (C-index) curves were utilized for the duration of 1–10 months in both cohorts. To correct multiple comparisons in functional enrichment analysis, the Benjamini-Hochberg method was applied to control the false discovery rate (FDR), and FDR-adjusted P-values (Q-values) were calculated.

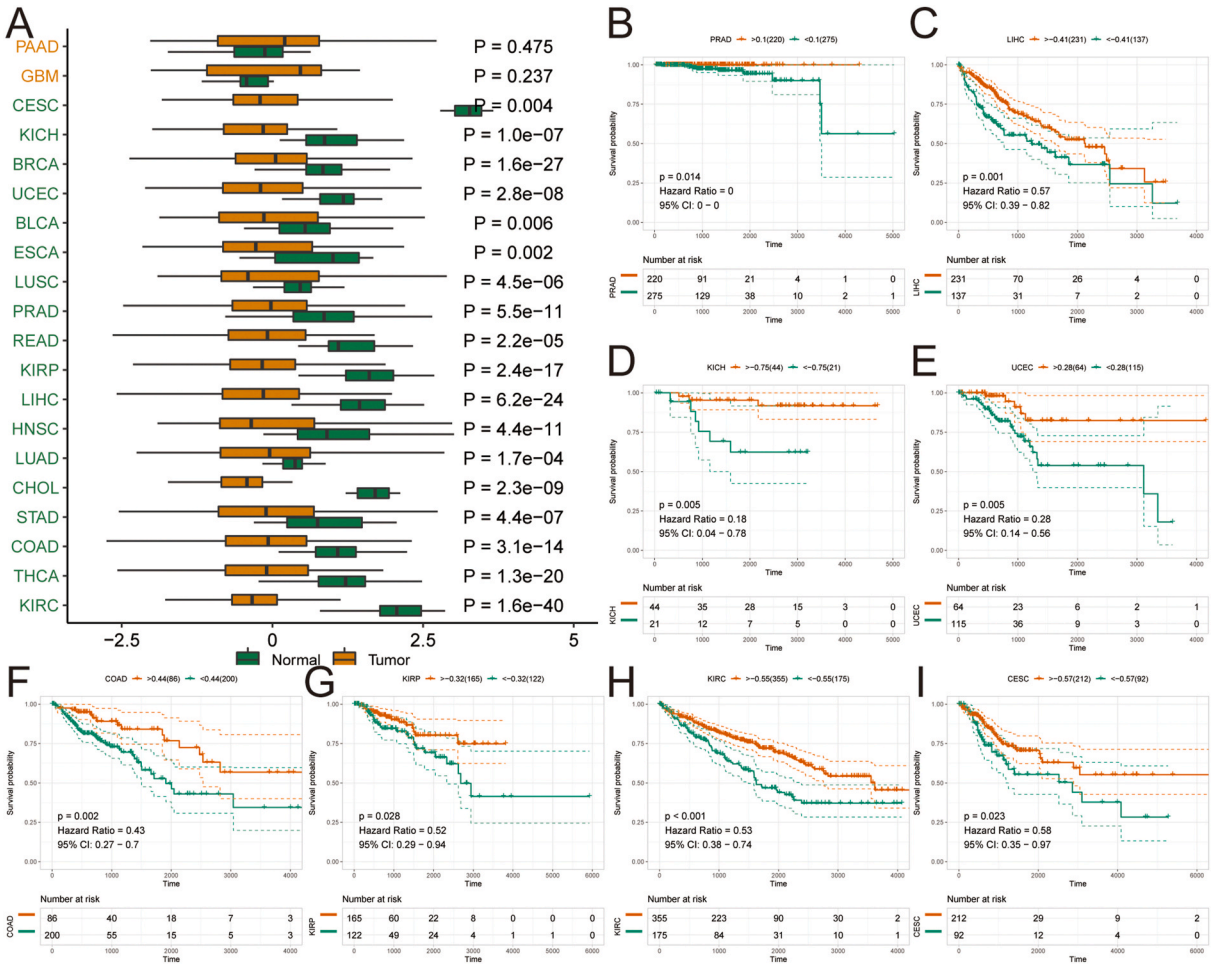

Fig. 1. The role of cuproptosis potential index (CPI) in Pan-cancer. (A) The differences of CPI, the modeled marker of cuproptosis, between tumor and normal tissues with wild type tumors. (B–I) Kaplan-Meier analysis of the low- and high-CFI in different tumors, such as PAAD (B), LIHC (C), KICH, (D), UCEC (E), CCAD (F), KIRP (G), KIRC (H), CESC (I).

4. Results

4.1. Pan-caner analysis of cuproptosis potential index (CPI)

A recent discovery has identified ten crucial genes, referred to as cuproptosis regulator genes (CRGs), that play a significant role in regulating cuproptosis. These genes include FDX1, LIPT1, DLD, LIAS, DLAT, PDHA1, PDHB, MTF1, GLS, and CDKN2A. To delve deeper into the understanding of the functional significance of cuproptosis in tumor development, progression, and metastasis, the cuproptosis potential index (CPI) was calculated. This metric was computed by subtracting the enrichment score (ES) of the negative core machine components from the ES of the positive ones, as quantified by ssGSEA. These calculations were performed using the ten CRGs within TCGA data. Subsequently, a comparison was conducted between tumor and normal tissues with wild type tumors, focusing on the differences in CPI, which serves as a modeled marker of cuproptosis (Fig. 1A). The findings revealed that, with the exception of pancreatic adenocarcinoma (PAAD) and glioblastoma multiforme (GBM), normal tissues exhibited significantly higher scores on the CFI compared to tumor tissues. Subsequently, the different tumor cohorts were divided into high-risk and low-risk groups based on the median CFI scores. The results demonstrated that patients with low-CFI scores experienced significantly longer overall survival compared to those with high-CFI scores in the PRAD, LIHC, KICH, UCEC, COAD, KIRP, KIRC, and CES (all $P < 0.05$, Fig. 1B–I). Our data presented that higher CFI are associated with faster tumor progression in these eight tumor types. Based on these findings, we chose HCC for further analysis.

4.2. Identification of CFI-related modules in WGCNA analysis

Initially, a differential analysis was conducted on TCGA-LIHC expression data, employing screening criteria of $|FC|>1$ and $FDR<0.05$. As a result, a comprehensive count of 5389 genes was effectively discerned. In order to identify the primary modules most closely linked to the CFI of hepatocellular carcinoma (HCC), we conducted a WGCNA using TCGA-LIHC dataset. Consequently, seven key modules were successfully derived. (Fig. 2A–B). Subsequently, we examined the associations between module eigengenes (MEs) and CFI. Notably, the blue module exhibited the strongest associations with CFI ($r = -0.56$, $P < 0.0001$) (Fig. 2C). The blue module

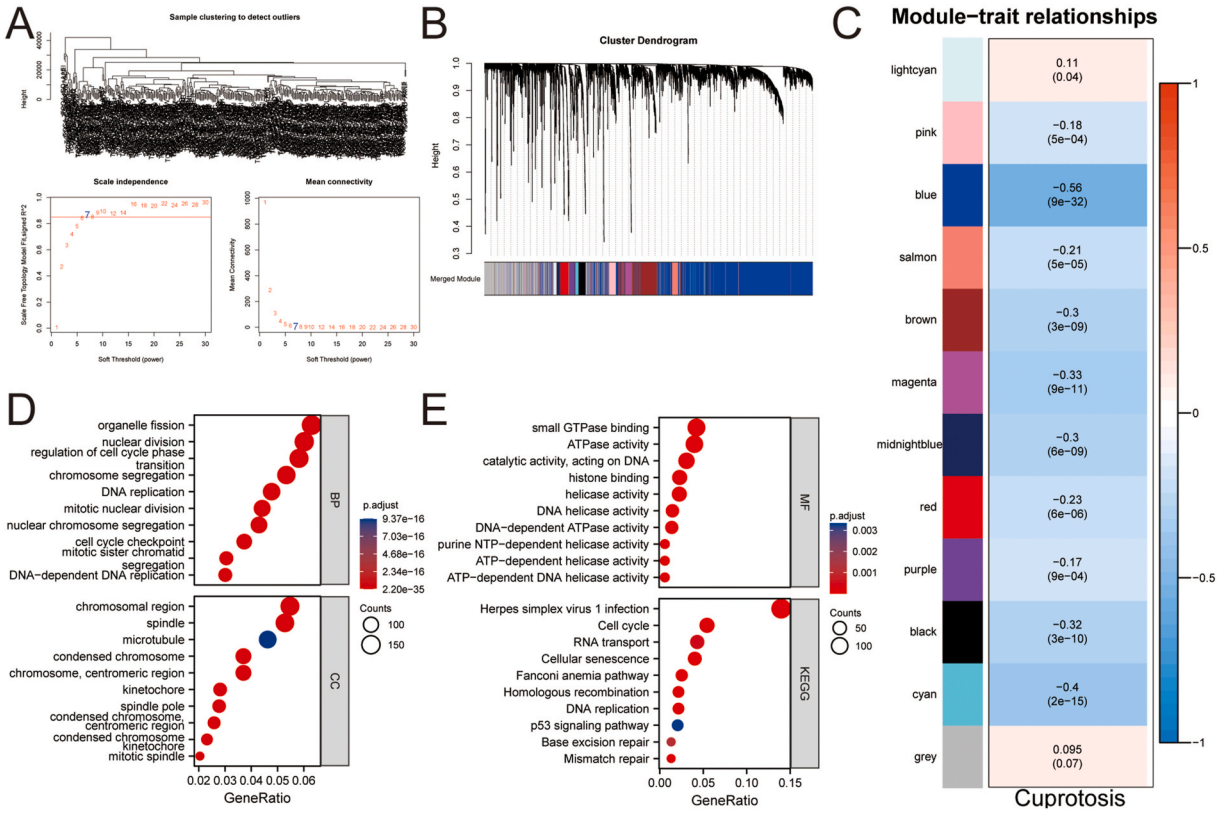

Fig. 2. Identification of modules and hub genes closely associated with clinical information of hepatocellular carcinoma (HCC) in RNA-seq data through WGCNA. (A) Analysis of the scale-free topology model fit index and mean connectivity across soft-thresholding powers. The most suitable power value was 7. (B) Gene module dendrogram constructed using a dissimilarity measure. (C) Diagram of the correlation between the module and the CFI. Each cell contains the corresponding correlation and *P* value. (D–E) GO and KEGG analysis identified the key biological processes (BP), molecular functions (MF), cellular components (CC), and pathways linked to high-risk genes in the lightcyan module.

was identified as the most crucial module in relation to the prognosis of CFI. Subsequently, genes within the blue module were selected for GO and KEGG analysis. The GO analysis highlighted key elements such as organelle fission, chromosomal region, and small GTPase binding (Fig. 2D and E). Additionally, the KEGG analysis identified key pathways, including RNA transport, Cellular senescence, and Fanconi anemia pathway, among others (Fig. 2E).

4.3. *Constructing the seven-gene signature*

Univariate Cox regression analysis was performed on the genes within the BLUE models to identify a total of 2055 genes with prognostic relevance (Fig. 3A). The top 10 genes were selected using the random survival forest variable hunting (RSFVH) algorithm, namely CBX2, TAF9, DHX37, FARSB, GNPDA1, TMEM69, SLC16A3, KIF20A, NOP58, and TCOF1 (Fig. 3B). Subsequently, Kaplan-Meier analysis was used to identify a risk signature consisting of a small number of genes with significant P-values (Fig. 3C). As a result, a seven-gene signature comprising TCOF1, NOP58, TMEM69, FARSB, DHX37, SLC16A3, and CBX2 emerged as the top-ranked

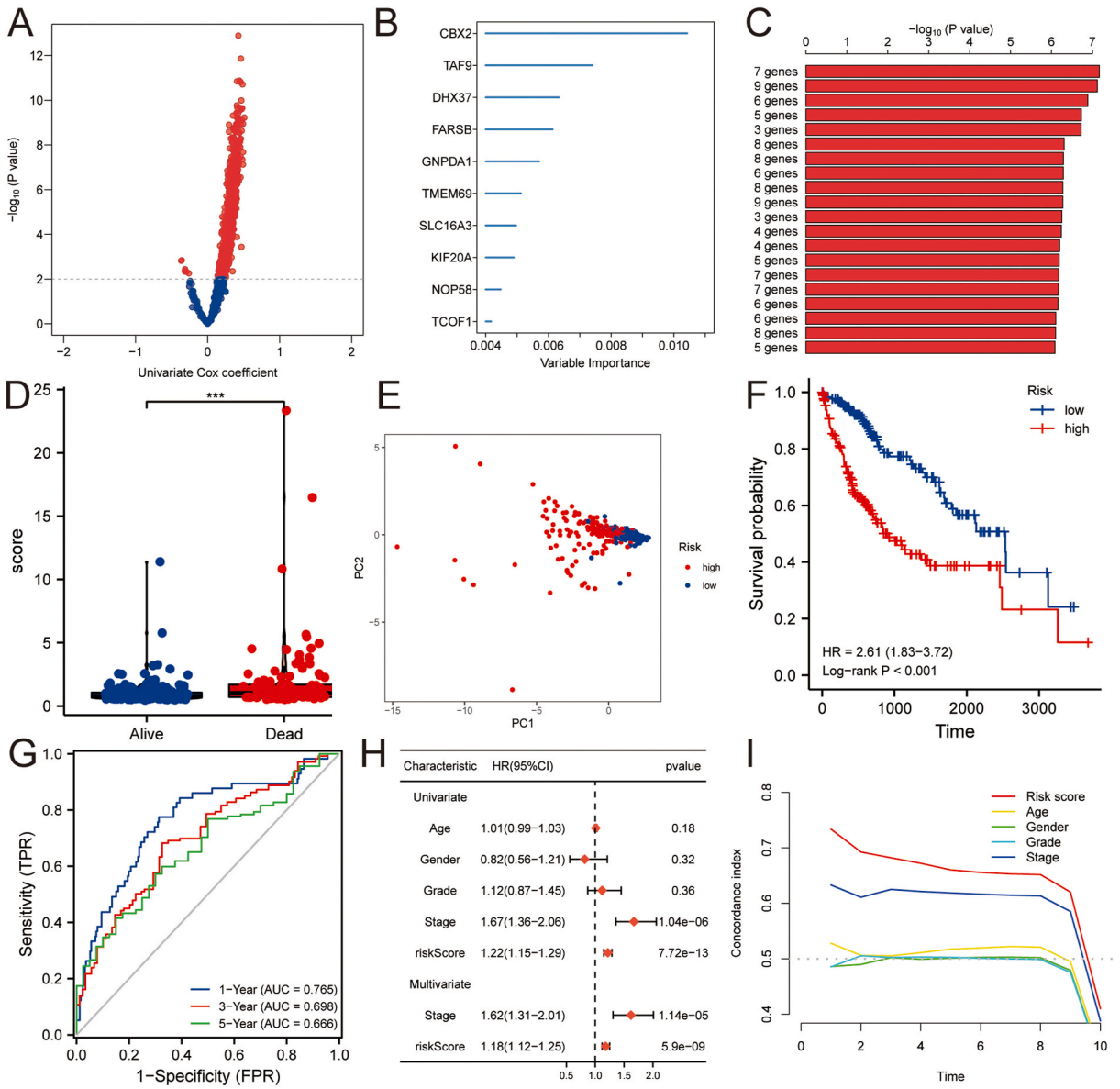

Fig. 3. Construction of the cuproptosis-related signature in TCGA cohort. (A) Volcano plot revealed DEGs in the red module. (B) A total of ten genes identified via random survival forest analysis (C) Top ten risk models based on the *P* value of Kaplan–Meier. (D–F) The high CFI score of the seven-gene signature showed high risk of death ($P < 0.05$). (G) Area under the curve (AUC) showed predictive accuracy of the risk model. (H) Univariate and multivariate Cox analysis evaluates risk model's prognostic value. (I) The time-dependent concordance-index (C-index) curves for 1–10 months.

signature. The seven-gene signature exhibited a high CFI score, indicating an elevated risk of mortality in HCC patients (Fig. 3D–F and Fig. 4A–C, respectively). To further assess the predictive capacity of this signature at different time points, the ROC analysis was conducted in both cohorts (Fig. 3G and 4D). The AUC values at 1-, 3-, and 5-year intervals for TCGA cohort were 0.765, 0.698, and 0.666, respectively (Fig. 3G), while ICGC cohort exhibited AUC values of 0.765, 0.768, and 0.867 at the same intervals (Fig. 4D). These findings suggest that the discovery of a powerful seven-gene signature that holds substantial prognostic value in HCC, with consistent predictive performance evidenced by high AUC values across multiple intervals in both TCGA and ICGC cohorts.

Univariate and multivariate Cox analyses were performed on clinical factors showing significance ($P < 0.05$) within TCGA (Fig. 3H) and ICGC (Fig. 4E) cohorts. The results affirmed that the risk score and clinical stage independently and significantly predict unfavorable outcomes in both groups. Additionally, time-dependent C-index curves were employed to assess the performance of the risk-score signature. The findings demonstrated that the risk-score signature had a superior effect compared to age, gender, and stage in TCGA (Fig. 3I) and ICGC (Fig. 4F) cohorts.

4.4. Examining the relationship between cuproptosis and clinical pathological factors

Given the intricate nature of the association between cuproptosis and HCC, we elucidated the correlation between the risk score and clinical pathological factors. The findings demonstrated that stages I&II had a correlation with a reduced risk score, while stages III&IV exhibited elevated risk scores (Fig. S1A). Additionally, the connection between the risk score and HCC grade suggested that grades 1&2 were linked to the lowest risk score, whereas grades 3&4 were associated with the highest risk score (Fig. S1B). The Sankey diagram provides a compelling visualization of the distribution of high and low risk scores of the cuproptosis-related signature and the survival status (alive or deceased) of HCC patients, highlighting a possible correlation between risk score and patient survival outcomes (Fig. S1C). Interestingly, patients with lower cuproptosis risk tended to have higher risk scores, while those with higher cuproptosis risk showed lower risk scores (Fig. S1D). These findings shed light on the interplay between cuproptosis and HCC risk, emphasizing the value of this risk score in patient stratification and prognosis. Similarly, the correlation between the Z score and the risk of cuproptosis highlighted that individuals exhibiting a lower risk of cuproptosis tend to have elevated Z scores in comparison to those with a higher risk of cuproptosis (Fig. S1E). The results obtained through the Kaplan-Meier method indicated that patients possessing low-risk scores exhibited considerably shorter overall survival (OS) in comparison to those with high-risk scores, irrespective of the Z score being low or high (Fig. S1F).

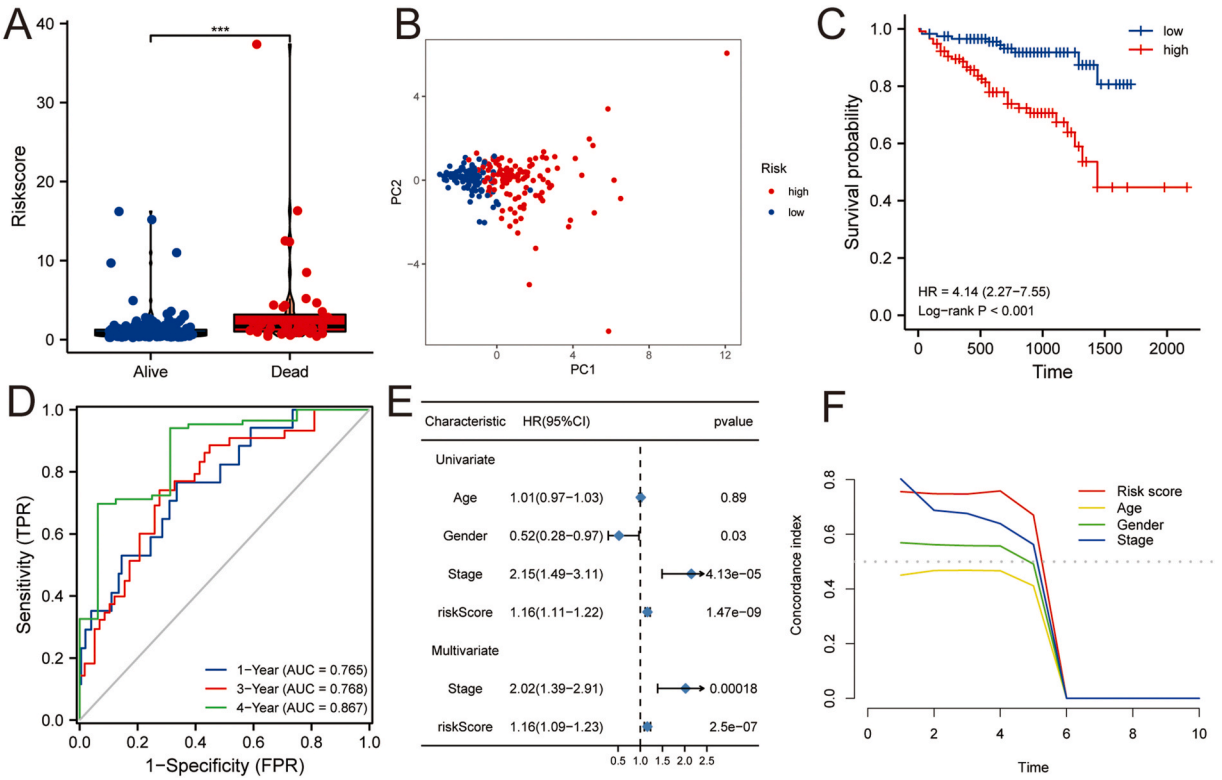

Fig. 4. The Signature-based risk score is validated in ICGC cohort. (A–C) The high CFI score of the seven-gene signature showed high risk of death ($P < 0.05$). (D) Area under the curve (AUC) showed predictive accuracy of the risk model. (E) Univariate and multivariate Cox analysis evaluates risk model's prognostic value. (F) The time-dependent concordance-index (C-index) curves for 1–10 months.

4.5. Analysis of immune cell infiltration

The CIBERSORT method was used to determine the relative proportions of various immune cell types in HCC, according to the different risk scores. In TCGA cohort, the score of "aDC", "NK CD56 bright cells", "T helper cells", "TFH", "Th2 cells" was elevated in the high-risk group; the score of "Cytoroxic cells", "DC", "Mast cells", "Neutrophils", "NK CD56 dim cells", "NK cells" et al. increased in the low-risk group (Fig. S2A). Fig. 6B illustrates that "CD274", "CD276", "TNFSF4", "CD27", "TNFSF15", "ICOS" et al. showed significantly increased values in the high-risk group (Fig. S2B). In TCGA database, "Type II IFN response", "Type I IFN response", and "MHC class I" were ranked as the most infiltrated immune cells (Fig. S2C). Furthermore, an examination of the risk scores among various immunotypes within TCGA database revealed that patients with type C3 exhibited the lowest risk score (Fig. S2D). Furthermore, an analysis of stem cell indices indicated that the high-risk group demonstrated significantly elevated stem cell characteristics (Fig. S2E).

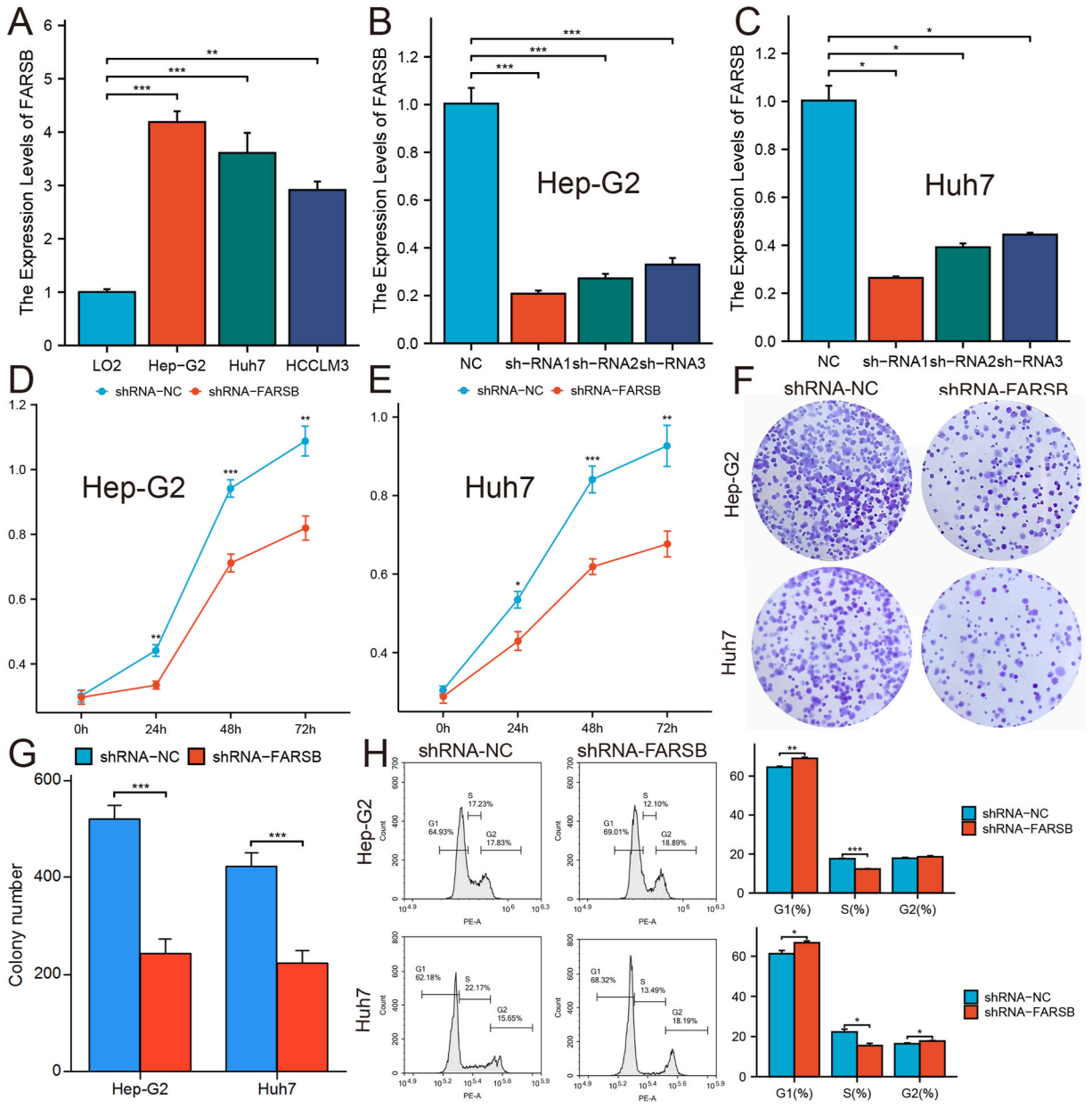

Fig. 5. FARSB knockdown affects HCC cell growth and cell cycle. (A) RT-PCR analysis of FARSB expression in various HCC and normal liver cells. Confirmation of efficient FARSB knockdown in Hep-G2 (B) and Huh7 (C) cells. Cell viability reduction in FARSB knockdown HepG2 (D) and Huh7 (E) cells via CCK-8 assay. (F, G) Clone formation assay for assessing cell proliferation ability in Huh7 and Hep-G2 cells. (H) Flow cytometry shows cell cycle arrest at G1 phase after FARSB knockdown.

4.6. Dissecting the correlation between tumor mutation burden and prognostic risk in HCC

Somatic mutation rates and A higher tumor mutation burden (TMB) are correlated with enhanced anti-cancer immune response [30]. The high-risk group (Fig. S3A) exhibited an average range of mutations per sample from 1 to 1200, while the low-risk group (Fig. S3B) displayed a range of 0–613 mutations. The waterfall plot visually represents the 20 most frequently mutated genes and

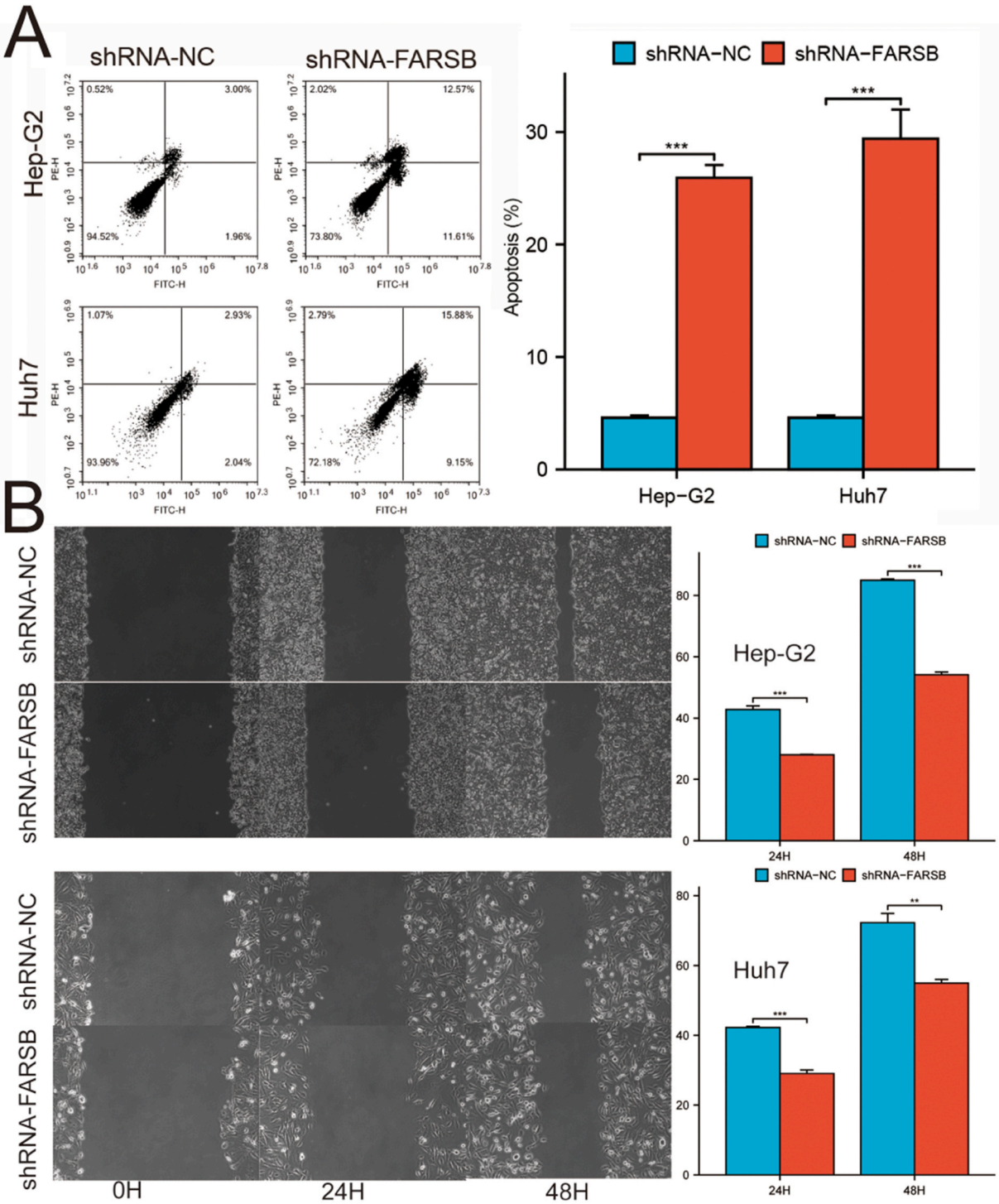

Fig. 6. Effect of FARSB on cell apoptosis and migration. (A) Increased apoptosis in FARSB knockdown HepG2 and Huh7 cells. (B) Wound-healing assay shows reduced migration in HepG2 and Huh7 cells after FARSB knockdown.

reveals the gene alterations present in 78.03 % (135 out of 173) of the high-risk group samples, and 64.41 % (114 out of 177) of the low-risk group samples (Figs. S3A and S3B). Within the high-risk group (Fig. S3A), the genes TP53, TTN, and MUC16 were the most commonly mutated, occurring in 41 %, 24 %, and 17 % of cases respectively. Comparatively, in the low-risk group (Fig. S3B), the most frequent mutations were observed in the genes TTN (22 %), TP53 (15 %), and MUC16 (12 %). Fig. S3C clearly illustrates that patients categorized with a high risk-score displayed significantly elevated TMB in comparison to those patients assigned a low risk-score ($P < 0.05$). Furthermore, in TCGA cohort, samples presenting TP53 mutations had notably higher risk scores compared to those of samples without such mutations (i.e., wild-type samples) (Fig. S3D, $P < 0.05$). In order to investigate the association among TMB, mutation status (wild type or mutant), and patient survival, the Kaplan-Meier analysis was conducted. The findings revealed that patients with a low TMB and wild type TP53 displayed a more promising outlook compared to those presenting a high TMB and mutant TP53 (Fig. S3E, $P < 0.001$).

4.7. Exploration of therapeutic drug sensitivity in relation to risk score signature

To explore the potential therapeutic drugs according to the risk score signature, we performed an analysis of drug sensitivity through the use of the GDSC website [29]. The outcomes indicated a notable variance in the sensitivity towards twelve compounds between the low- and high-risk groups. Six specific compounds (Axitinib, ZAD.0530, AP.24534, AMG.706, AKT. inhibitor. VIII and AICAR) demonstrated increased sensitivity in the high-risk group (Fig. S4A). Conversely, another set of six compounds (AZ628, AUY922, ATRA, AS601245, AG.014699 and ABT.888) exhibited heightened sensitivity in the low-risk group (Fig. S4B).

4.8. Functional annotation and pathway analysis

We utilized a GSEA analysis to identify key enrichment pathways in connection with the high and low risk groups. Pathways involving cell cycle processes, DNA replication, receptor interaction, lipid metabolism, and neuroactive ligand receptor interaction displayed a notable enrichment in the high-risk group (Fig. S5A). On the flip side, the low-risk group manifested a pronounced enrichment in pathways tied to complement and coagulation cascades, cytochrome P450 metabolism, fatty acid metabolism, metabolism of glycine, serine and threonine, retinol metabolism (Fig. S5B).

4.9. Development and validation of a nomogram for predicting OS in HCC patients

In order to develop a practical approach for predicting the OS of patients suffering from HCC, we devised a nomogram incorporating both risk score and pathological stage (Fig. S6A). Following this, a calibration curve was employed to evaluate the accuracy of our model. The observed 1-year, 3-year, and 5-year survival rates closely matched the predictions of the nomogram, confirming the model's reliability (Fig. S6B). The ROC curve analysis further underscored the efficacy of the nomogram, which exhibited the highest AUC when integrating both risk score and pathological stage. Additionally, the AUC values for the survival predictions at 1, 3, and 5 years were greater than 0.69, suggesting that our prognostic model, integrating both risk scores and pathological stages, offers a better predictive performance than a model relying on a single prognostic factor. This result is depicted in Fig. S6C and indicates the utility of our nomogram as an effective instrument for predicting survival outcomes in HCC patients.

4.10. Exploring the impact of FARSB expression on HCC cell behavior and functionality

We used RT-PCR analysis and found significantly increased FARSB expression levels in HCC cell lines HepG2, Huh7, and HCCLM3, in contrast to normal liver cells (Fig. 5A). This was further validated by Western blot analysis indicating amplified FARSB presence in HCC cells (Fig. S7A). In order to assess the impact of FARSB on cell growth, HepG2 and Huh7 cells were transduced with three short hairpin RNA (shRNA) molecules targeting FARSB (Fig. 5B, C, S7B). A clear reduction in the viability of HepG2 and Huh7 cells subjected to FARSB depletion was observed, evidenced by the CCK-8 assays (Fig. 5D and E). Additionally, colony-formation assay indicated that clonogenic potential was decreased after FARSB knockdown (Fig. 5F and G), flow cytometry analysis demonstrated a noteworthy reduction in cells residing in the S phase, concomitant with an elevation in cells occupying the G1 phase, thereby implying a potential G1 phase arrest (Fig. 5H). Moreover, an increase in the number of apoptotic cells was also noted, suggesting an augmentation of the apoptotic process post-FARSB inhibition (Fig. 6A), following knockdown of FARSB in HepG2 and Huh7 cells, wound-healing assays provided evidence that the knockdown of FARSB substantially impeded the migratory capabilities of HepG2 and Huh7 cells (Fig. 6B).

5. Discussion

Copper (Cu), an element crucial for vital biological processes [31], can trigger various forms of cell death such as apoptosis and autophagy [32]. Nowadays, cuproptosis, a non-apoptotic form of programmed cell death induced by an overabundance of copper, is just now coming into focus [22]. Other studies have also shed light on the complex interplay between various forms of cell death and tumor growth [33,34]. Our study brings to light the crucial importance of cuproptosis in the pathophysiology of HCC. In our research, we have provided a comprehensive description of the clinical significance of cuproptosis patterns in HCC and their potential association with TMB characteristics. Furthermore, we have proposed a cuproptosis scoring system to assess individual cuproptosis levels, aiming to enhance the comprehension of TMB and aid physicians in devising more efficacious immunotherapeutic approaches.

The initial phase of our study involved the evaluation of the CPI, a recognized indicator of cuproptosis, across diverse cancer types.

Our results revealed that, in general, normal tissues exhibited higher CPI scores in comparison to tumor tissues, except for pancreatic adenocarcinoma and glioblastoma multiforme. Furthermore, heightened CPI scores were observed to be correlated with accelerated tumor progression in eight cancer types, suggesting a potential association between increased cuproptosis and unfavorable cancer outcomes. Consistent with prior investigations, a majority of the copper-utilizing genes (CUGs), including CDKN2A, were found to be altered. Our analysis incorporated ssGSEA and GSVA to reveal the hallmark pathways and biological significance among aging phenotypes. Previous research also affirms the significant role of gene expression profiling in cancer prognosis and therapy [35,36].

Our nomogram, which combines risk index and disease stage, underscores the efficacy of our risk score as a reliable and precise instrument for HCC patients. This model builds upon and adds complexity to prior prognostic models based on the TNM staging system or single biomarker. Our model achieved an AUC above 0.69 for survival prediction, outperforming models relying on single prognostic factors. The findings parallel recent advances in the field of prognostic modeling in oncology, underscoring the need for multifactorial risk assessment.

The biological processes associated with the risk score revealed an intricate interaction between cuproptosis and immune response in HCC, hinting at the potential involvement of the immune system in cuproptosis-mediated cancer progression. This understanding could guide the development of new immunotherapy strategies for treating HCC [37]. Through tumor mutational burden (TMB) and somatic mutation analysis, we also noted a relationship between high risk-score patients, TP53 mutations, and higher TMB, all of which correlated with a worse prognosis. This observation is in line with the known role of TP53 mutations in promoting tumorigenesis and contributing to poor prognosis in various types of cancer. Additionally, our research revealed potential therapeutic agents targeting high and low-risk HCC patients, which could guide precision medicine in HCC treatment. By predicting potential compounds for HCC therapy using the GDSC database and calculating the IC50 values, we were able to provide insights into possible therapeutic interventions for HCC [38].

The most striking finding of our study is the differential sensitivity to various chemical compounds observed in HCC groups, as defined by our signature. The high-risk group exhibited greater sensitivity to six compounds: Axitinib, ZAD.0530, AP.24534, AMG.706, AKT. inhibitor. VIII, and AICAR. Conversely, the low-risk group showed a heightened response to AZ628, AUY922, ATRA, AS601245, AG.014699, and ABT.888. These findings are reminiscent of the work of Garnett et al. (2013), who explored the relationship between cancer genomics and drug sensitivity [29]. Our study extends this concept to a risk-stratified context, with promising implications for personalized treatment in HCC.

Finally, we demonstrated that knockdown of FARSB, one of the genes included in our six-gene signature, in HCC cells led to decreased cell viability, cell cycle arrest, enhanced apoptosis, and inhibited migration and invasion *in vitro*, further supporting the potential prognostic and therapeutic relevance of the identified genes. This finding is congruous with previous literature demonstrating aberrant expression of FARSB in various types of malignancies. For example, a study by Gao et al. illustrated that FARSB is significantly upregulated in gastric cancer, promoting tumor progression [39]. Similarly, a study by Zhang underscores FARSB's influence in promoting an immunosuppressive 'cold' tumor microenvironment across 25 different types of tumors, highlighting its potential as a novel biomarker for assessing the immunotherapeutic response [40]. Our findings extend these observations to HCC and provide further evidence that FARSB could potentially have a significant part in driving the development of HCC.

In the context of current research, our seven-gene signature, which includes key genes such as FARSB, provides unique insights compared to existing prognostic models. Unlike traditional markers, our signature incorporates aspects of cuproptosis, offering a more comprehensive understanding of tumor biology in hepatocellular carcinoma (HCC). This integrative approach not only supports its prognostic value but also illuminates potential targets for therapeutic intervention. This distinct focus on regulated cell death mechanisms sets our model apart from earlier studies, which typically do not emphasize these pathways.

Considering the practical application of our seven-gene signature in clinical settings, it is imperative to discuss how it could be integrated into existing diagnostic workflows. Such integration poses several challenges, including the need for standardized and robust assay methods to accurately measure gene expression levels in clinical samples. Moreover, implementing this signature will require interdisciplinary collaboration to ensure the data are interpreted effectively within the context of individual patient care plans. Additionally, the economic and logistical implications of adopting such advanced diagnostic tools in routine practice must be considered, assessing the balance between cost and potential improvement in patient outcomes.

Despite our insightful findings, additional experimental and clinical validation are required to substantiate these associations, and to uncover the underlying mechanisms that govern the interaction between cuproptosis, cancer progression, and immunity. To further enhance the robustness of our findings, future studies should investigate the impact of additional potential confounders such as patient demographics, underlying comorbidities, and genetic background, which were beyond the scope of the current study. Addressing these factors is crucial to fully understand the applicability and effectiveness of the cuproptosis-related risk model in diverse patient populations.

In conclusion, this research outlines a prognostic signature for HCC based on cuproptosis as a valuable tool for prognostic prediction, therapeutic guidance, and understanding the immune landscape in HCC. And our study and prior literature underline the pivotal function of FARSB in the genesis and advancement of cancer. Despite the promising findings, future investigation is necessary to solidify the clinical applicability of our model.

Ethics approval and consent to participate

Not applicable.

Consent for publication

All authors gave their consent for publication.

Data availability statement

The data used in this study are derived from publicly available datasets. Specifically, the data were obtained from The Cancer Genome Atlas (TCGA) and the International Cancer Genome Consortium (ICGC). Access to TCGA data can be facilitated through the Genomic Data Commons (GDC) Data Portal, available at https://portal.gdc.cancer.gov/. Similarly, the ICGC data are accessible via the ICGC Data Portal, which can be found at https://dcc.icgc.org/. Both datasets are publicly available and can be accessed without restrictions.

Funding

The present study received financial support from the National Natural Science Foundation of China (82204909).

CRediT authorship contribution statement

Junlin Duan: Writing – original draft, Software, Investigation, Data curation. **Xuan Zhang:** Validation, Resources, Formal analysis. **Jingyu Xu:** Visualization, Methodology, Data curation. **Jun Liu:** Writing – review & editing, Methodology, Investigation, Formal analysis, Data curation. **Hetong Zhao:** Writing – review & editing, Investigation, Funding acquisition, Conceptualization.

Declaration of competing interest

The authors declare that they have no known competing financial interests or personal relationships that could have appeared to influence the work reported in this paper.

Acknowledgements

Not applicable.

Appendix A. Supplementary data

Supplementary data to this article can be found online at https://doi.org/10.1016/j.heliyon.2024.e32289.

References

[1] T. Akinyemiju, S. Abera, M. Ahmed, N. Alam, M.A. Alemayohu, C. Allen, R. Al-Raddadi, N. Alvis-Guzman, Y. Amoako, A. Artaman, T.A. Ayele, A. Barac, I. Bensenor, A. Berhane, Z. Bhutta, J. Castillo-Rivas, A. Chitheer, J.Y. Choi, B. Cowie, L. Dandona, R. Dandona, S. Dey, D. Dicker, H. Phuc, D.U. Ekwueme, M. S. Zaki, F. Fischer, T. Fürst, J. Hancock, S.I. Hay, P. Hotez, S.H. Jee, A. Kasaeian, Y. Khader, Y.H. Khang, A. Kumar, M. Kutz, H. Larson, A. Lopez, R. Lunevicius, R. Malekzadeh, C. McAlinden, T. Meier, W. Mendoza, A. Mokdad, M. Moradi-Lakeh, G. Nagel, Q. Nguyen, G. Nguyen, F. Ogbo, G. Patton, D.M. Pereira, F. Pourmalek, M. Qorbani, A. Radfar, G. Roshandel, J.A. Salomon, J. Sanabria, B. Sartorius, M. Satpathy, M. Sawhney, S. Sepanlou, K. Shackelford, H. Shore, J. Sun, D.T. Mengistu, R. Topór-Mądry, B. Tran, K.N. Ukwaja, V. Vlassov, S.E. Vollset, T. Vos, T. Wakayo, E. Weiderpass, A. Werdecker, N. Yonemoto, M. Younis, C. Yu, Z. Zaidi, L. Zhu, C.J.L. Murray, M. Naghavi, C. Fitzmaurice, The burden of primary liver cancer and underlying etiologies from 1990 to 2015 at the global, regional, and national level: results from the global burden of disease study 2015, JAMA Oncol. 3 (2017), https://doi.org/10.1001/jamaoncol.2017.3055.

[2] H. Sung, J. Ferlay, R.L. Siegel, M. Laversanne, I. Soerjomataram, A. Jemal, F. Bray, Global cancer statistics 2020: GLOBOCAN estimates of incidence and mortality worldwide for 36 cancers in 185 countries, CA A Cancer J. Clin. 71 (2021), https://doi.org/10.3322/caac.21660.

[3] Y. Lu, Y.T. Chan, J. Wu, Z. Feng, H. Yuan, Q. Li, T. Xing, L. Xu, C. Zhang, H.Y. Tan, T.K. Lee, Y. Feng, N. Wang, CRISPR/Cas9 screens unravel miR-3689a-3p regulating sorafenib resistance in hepatocellular carcinoma via suppressing CCS/SOD1-dependent mitochondrial oxidative stress, Drug Resist. Updates 71 (2023), https://doi.org/10.1016/j.drup.2023.101015.

[4] S. Wang, L. Zhou, N. Ji, C. Sun, L. Sun, J. Sun, Y. Du, N. Zhang, Y. Li, W. Liu, W. Lu, Targeting ACYP1-mediated glycolysis reverses lenvatinib resistance and restricts hepatocellular carcinoma progression, Drug Resist. Updates 69 (2023), https://doi.org/10.1016/j.drup.2023.100976.

[5] H. Hu, Q. Xu, Z. Mo, X. Hu, Q. He, Z. Zhang, Z. Xu, New anti-cancer explorations based on metal ions, J. Nanobiotechnol. 20 (2022), https://doi.org/10.1186/s12951-022-01661-w.

[6] F. Bu, X. Li, Y. Zhao, L. Bai, S. Zhang, L. Min, Pan-cancer patterns of cuproptosis markers reveal biologically and clinically relevant cancer subtypes, Biomark. Res. 11 (2023), https://doi.org/10.1186/s40364-022-00446-5.

[7] H.W. Kuo, S.F. Chen, C.C. Wu, D.R. Chen, J.H. Lee, Serum and tissue trace elements in patients with breast cancer in Taiwan, Biol. Trace Elem. Res. 89 (2002), https://doi.org/10.1385/BTER:89:1:1.

[8] C.I. Davis, X. Gu, R.M. Kiefer, M. Ralle, T.P. Gade, D.C. Brady, Altered copper homeostasis underlies sensitivity of hepatocellular carcinoma to copper chelation, Metallomics 12 (2020), https://doi.org/10.1039/d0mt00156b.

[9] M. Diez, M. Arroyo, F.J. Cerdan, M. Munoz, M.A. Martin, J.L. Balibrea, Serum and tissue trace metal levels in lung cancer, Oncology 46 (1989), https://doi.org/10.1159/000226722.

[10] Y. Li, Copper homeostasis: emerging target for cancer treatment, IUBMB Life 72 (2020), https://doi.org/10.1002/iub.2341.

[11] Z. Wang, D. Jin, S. Zhou, N. Dong, Y. Ji, P. An, J. Wang, Y. Luo, J. Luo, Regulatory roles of copper metabolism and cuproptosis in human cancers, Front. Oncol. 13 (2023), https://doi.org/10.3389/fonc.2023.1123420.

[12] P. Lelievre, L. Sancey, J.L. Coll, A. Deniaud, B. Busser, The multifaceted roles of copper in cancer: a trace metal element with dysregulated metabolism, but also a target or a bullet for therapy, Cancers 12 (2020), https://doi.org/10.3390/cancers12123594.

[13] Y. Xue, X. Jiang, J. Wang, Y. Zong, Z. Yuan, S. Miao, X. Mao, Effect of regulatory cell death on the occurrence and development of head and neck squamous cell carcinoma, Biomark. Res. 11 (2023), https://doi.org/10.1186/s40364-022-00433-w.

[14] H. Guo, Y. Ouyang, H. Yin, H. Cui, H. Deng, H. Liu, Z. Jian, J. Fang, Z. Zuo, X. Wang, L. Zhao, Y. Zhu, Y. Geng, P. Ouyang, Induction of autophagy via the ROS-dependent AMPK-mTOR pathway protects copper-induced spermatogenesis disorder, Redox Biol. 49 (2022), https://doi.org/10.1016/j.redox.2021.102227.

[15] D. Guan, L. Zhao, X. Shi, X. Ma, Z. Chen, Copper in cancer: from pathogenesis to therapy, Biomed. Pharmacother. 163 (2023), https://doi.org/10.1016/j.biopha.2023.114791.

[16] D. Yoshida, Y. Ikeda, S. Nakazawa, Quantitative analysis of copper, zinc and copper/zinc ratio in selected human brain tumors, J. Neuro Oncol. 16 (1993), https://doi.org/10.1007/BF01324697.

[17] R. Safi, E.R. Nelson, S.K. Chitneni, K.J. Franz, D.J. George, M.R. Zalutsky, D.P. McDonnell, Copper signaling axis as a target for prostate cancer therapeutics, Cancer Res. 74 (2014), https://doi.org/10.1158/0008-5472.CAN-13-3527.

[18] J.H. Lefkowitch, R. Muschel, J.B. Price, C. Marboe, S. Braunhut, Copper and copper-binding protein in fibrolamellar liver cell carcinoma, Cancer 51 (1983), https://doi.org/10.1002/1097-0142(19830101)51:1<97::aid-cncr2820510120>3.0.co.

[19] F. Tisato, C. Marzano, M. Porchia, M. Pellei, C. Santini, Copper in diseases and treatments, and copper-based anticancer strategies, Med. Res. Rev. 30 (2010), https://doi.org/10.1002/med.20174.

[20] D. Zheng, J. Liu, H. Piao, Z. Zhu, R. Wei, K. Liu, ROS-triggered endothelial cell death mechanisms: focus on pyroptosis, parthanatos, and ferroptosis, Front. Immunol. 13 (2022), https://doi.org/10.3389/fimmu.2022.1039241.

[21] D. Bertheloot, E. Latz, B.S. Franklin, Necroptosis, pyroptosis and apoptosis: an intricate game of cell death, Cell. Mol. Immunol. 18 (2021), https://doi.org/10.1038/s41423-020-00630-3.

[22] P. Tsvetkov, S. Coy, B. Petrova, M. Dreishpoon, A. Verma, M. Abdusamad, J. Rossen, L. Joesch-Cohen, R. Humeidi, R.D. Spangler, J.K. Eaton, E. Frenkel, M. Kocak, S.M. Corsello, S. Lutsenko, N. Kanarek, S. Santagata, T.R. Golub, Copper induces cell death by targeting lipoylated TCA cycle proteins, Science (New York, N.Y.) (2022) 375, https://doi.org/10.1126/science.abf0529.

[23] G. Zhong, L. Li, Y. Li, F. Ma, J. Liao, Y. Li, H. Zhang, J. Pan, L. Hu, Z. Tang, Cuproptosis is involved in copper-induced hepatotoxicity in chickens, Sci. Total Environ. 866 (2023), https://doi.org/10.1016/j.scitotenv.2023.161458.

[24] Y. Wang, Y. Chen, J. Zhang, Y. Yang, J.S. Fleishman, Y. Wang, J. Wang, J. Chen, Y. Li, H. Wang, Cuproptosis: a novel therapeutic target for overcoming cancer drug resistance, Drug Resist. Updates 72 (2024), https://doi.org/10.1016/j.drup.2023.101018.

[25] S. Hänzelmann, R. Castelo, J. Guinney, GSVA: gene set variation analysis for microarray and RNA-seq data, BMC Bioinf. 14 (2013), https://doi.org/10.1186/1471-2105-14-7.

[26] G. Yu, L.G. Wang, Y. Han, Q.Y. He, clusterProfiler: an R package for comparing biological themes among gene clusters, OMICS A J. Integr. Biol. 16 (2012), https://doi.org/10.1089/omi.2011.0118.

[27] A.M. Newman, C.L. Liu, M.R. Green, A.J. Gentles, W. Feng, Y. Xu, C.D. Hoang, M. Diehn, A.A. Alizadeh, Robust enumeration of cell subsets from tissue expression profiles, Nat. Methods 12 (2015), https://doi.org/10.1038/nmeth.3337.

[28] Z.R. Chalmers, C.F. Connelly, D. Fabrizio, L. Gay, S.M. Ali, R. Ennis, A. Schrock, B. Campbell, A. Shlien, J. Chmielecki, F. Huang, Y. He, J. Sun, U. Tabori, M. Kennedy, D.S. Lieber, S. Roels, J. White, G.A. Otto, J.S. Ross, L. Garraway, V.A. Miller, P.J. Stephens, G.M. Frampton, Analysis of 100,000 human cancer genomes reveals the landscape of tumor mutational burden, Genome Med. 9 (2017), https://doi.org/10.1186/s13073-017-0424-2.

[29] W. Yang, J. Soares, P. Greninger, E.J. Edelman, H. Lightfoot, S. Forbes, N. Bindal, D. Beare, J.A. Smith, I.R. Thompson, S. Ramaswamy, P.A. Futreal, D.A. Haber, M.R. Stratton, C. Benes, U. McDermott, M.J. Garnett, Genomics of Drug Sensitivity in Cancer (GDSC): a resource for therapeutic biomarker discovery in cancer cells, Nucleic Acids Res. 41 (2013), https://doi.org/10.1093/nar/gks1111.

[30] M.S. Rooney, S.A. Shukla, C.J. Wu, G. Getz, N. Hacohen, Molecular and genetic properties of tumors associated with local immune cytolytic activity, Cell 160 (2015), https://doi.org/10.1016/j.cell.2014.12.033.

[31] T. Tsang, C.I. Davis, D.C. Brady, Copper biology, Curr. Biol. : CB 31 (2021), https://doi.org/10.1016/j.cub.2021.03.054.

[32] Y. Jiang, Z. Huo, X. Qi, T. Zuo, Z. Wu, Copper-induced tumor cell death mechanisms and antitumor theragnostic applications of copper complexes, Nanomedicine (London, England) (2022) 17, https://doi.org/10.2217/nnm-2021-0374.

[33] L. Galluzzi, I. Vitale, S.A. Aaronson, J.M. Abrams, D. Adam, P. Agostinis, E.S. Alnemri, L. Altucci, I. Amelio, D.W. Andrews, M. Annicchiarico-Petruzzelli, A. V. Antonov, E. Arama, E.H. Baehrecke, N.A. Barlev, N.G. Bazan, F. Bernassola, M.J.M. Bertrand, K. Bianchi, M.V. Blagosklonny, K. Blomgren, C. Borner, P. Boya, C. Brenner, M. Campanella, E. Candi, D. Carmona-Gutierrez, F. Cecconi, F.K. Chan, N.S. Chandel, E.H. Cheng, J.E. Chipuk, J.A. Cidlowski, A. Ciechanover, G. M. Cohen, M. Conrad, J.R. Cubillos-Ruiz, P.E. Czabotar, V. D'Angiolella, T.M. Dawson, V.L. Dawson, V. De Laurenzi, R. De Maria, K.M. Debatin, R. J. DeBerardinis, M. Deshmukh, N. Di Daniele, F. Di Virgilio, V.M. Dixit, S.J. Dixon, C.S. Duckett, B.D. Dynlacht, W.S. El-Deiry, J.W. Elrod, G.M. Fimia, S. Fulda, A.J. García-Sáez, A.D. Garg, C. Garrido, E. Gavathiotis, P. Golstein, E. Gottlieb, D.R. Green, L.A. Greene, H. Gronemeyer, A. Gross, G. Hajnoczky, J.M. Hardwick, I.S. Harris, M.O. Hengartner, C. Hetz, H. Ichijo, M. Jäättelä, B. Joseph, P.J. Jost, P.P. Juin, W.J. Kaiser, M. Karin, T. Kaufmann, O. Kepp, A. Kimchi, R.N. Kitsis, D. J. Klionsky, R.A. Knight, S. Kumar, S.W. Lee, J.J. Lemasters, B. Levine, A. Linkermann, S.A. Lipton, R.A. Lockshin, C. López-Otín, S.W. Lowe, T. Luedde, E. Lugli, M. MacFarlane, F. Madeo, M. Malewicz, W. Malorni, G. Manic, J.C. Marine, S.J. Martin, J.C. Martinou, J.P. Medema, P. Mehlen, P. Meier, S. Melino, E.A. Miao, J.D. Molkentin, U.M. Moll, C. Muñoz-Pinedo, S. Nagata, G. Nuñez, A. Oberst, M. Oren, M. Overholtzer, M. Pagano, T. Panaretakis, M. Pasparakis, J. M. Penninger, D.M. Pereira, S. Pervaiz, M.E. Peter, M. Piacentini, P. Pinton, J.H.M. Prehn, H. Puthalakath, G.A. Rabinovich, M. Rehm, R. Rizzuto, C.M. P. Rodrigues, D.C. Rubinsztein, T. Rudel, K.M. Ryan, E. Sayan, L. Scorrano, F. Shao, Y. Shi, J. Silke, H.U. Simon, A. Sistigu, B.R. Stockwell, A. Strasser, G. Szabadkai, S.W.G. Tait, D. Tang, N. Tavernarakis, A. Thorburn, Y. Tsujimoto, B. Turk, T. Vanden Berghe, P. Vandenabeele, M.G. Vander Heiden, A. Villunger, H.W. Virgin, K.H. Vousden, D. Vucic, E.F. Wagner, H. Walczak, D. Wallach, Y. Wang, J.A. Wells, W. Wood, J. Yuan, Z. Zakeri, B. Zhivotovsky, L. Zitvogel, G. Melino, G. Kroemer, Molecular mechanisms of cell death: recommendations of the nomenclature committee on cell death 2018, Cell Death Differ. 25 (2018), https://doi.org/10.1038/s41418-017-0012-4.

[34] D. Tang, R. Kang, T.V. Berghe, P. Vandenabeele, G. Kroemer, The molecular machinery of regulated cell death, Cell Res. 29 (2019), https://doi.org/10.1038/s41422-019-0164-5.

[35] Comprehensive and Integrative Genomic Characterization of Hepatocellular Carcinoma, Cell 169 (2017), https://doi.org/10.1016/j.cell.2017.05.046.

[36] W. Li, J. Liu, D. Zhang, L. Gu, H. Zhao, The prognostic significance and potential mechanism of ferroptosis-related genes in hepatocellular carcinoma, Front. Genet. 13 (2022), https://doi.org/10.3389/fgene.2022.844624.

[37] X.Y. Huang, F. Li, T.T. Li, J.T. Zhang, X.J. Shi, X.Y. Huang, J. Zhou, Z.Y. Tang, Z.L. Huang, A clinically feasible circulating tumor cell sorting system for monitoring the progression of advanced hepatocellular carcinoma, J. Nanobiotechnol. 21 (2023), https://doi.org/10.1186/s12951-023-01783-9.

[38] M.J. Garnett, E.J. Edelman, S.J. Heidorn, C.D. Greenman, A. Dastur, K.W. Lau, P. Greninger, I.R. Thompson, X. Luo, J. Soares, Q. Liu, F. Iorio, D. Surdez, L. Chen, R.J. Milano, G.R. Bignell, A.T. Tam, H. Davies, J.A. Stevenson, S. Barthorpe, S.R. Lutz, F. Kogera, K. Lawrence, A. McLaren-Douglas, X. Mitropoulos, T. Mironenko, H. Thi, L. Richardson, W. Zhou, F. Jewitt, T. Zhang, P. O'Brien, J.L. Boisvert, S. Price, W. Hur, W. Yang, X. Deng, A. Butler, H.G. Choi, J.W. Chang, J. Baselga, I. Stamenkovic, J.A. Engelman, S.V. Sharma, O. Delattre, J. Saez-Rodriguez, N.S. Gray, J. Settleman, P.A. Futreal, D.A. Haber, M.R. Stratton, S. Ramaswamy, U. McDermott, C.H. Benes, Systematic identification of genomic markers of drug sensitivity in cancer cells, Nature 483 (2012), https://doi.org/10.1038/nature11005.

[39] X. Gao, R. Guo, Y. Li, G. Kang, Y. Wu, J. Cheng, J. Jia, W. Wang, Z. Li, A. Wang, H. Xu, Y. Jia, Y. Li, X. Qi, Z. Wei, C. Wei, Contribution of upregulated aminoacyl-tRNA biosynthesis to metabolic dysregulation in gastric cancer, J. Gastroenterol. Hepatol. 36 (2021), https://doi.org/10.1111/jgh.15592.

[40] Z. Zhang, J. Tan, Z. Yu, C. Liu, J. Wang, D. Wu, X. Bai, [FARSB stratifies prognosis and cold tumor microenvironment across different cancer types: an integrated single cell and bulk RNA sequencing analysis], Nan fang yi ke da xue xue bao = Journal of Southern Medical University 43 (2023), https://doi.org/10.12122/j.issn.1673-4254.2023.05.01.